JCI insight

Primary tumors induce neutrophil extracellular traps with targetable metastasis promoting effects

Roni F. Rayes, … , Lorenzo E. Ferri, Jonathan D. Spicer

JCI Insight. 2019. https://doi.org/10.1172/jci.insight.128008.

Research In-Press Preview **Oncology**

Targeting the dynamic tumor immune microenvironment (TIME) can provide effective therapeutic strategies for cancer. Neutrophils are the predominant leukocyte population in mice and humans, and mounting evidence implicates these cells during tumor growth and metastasis. Neutrophil extracellular traps (NETs) are networks of extracellular neutrophil DNA fibers that are capable of binding tumor cells to support metastatic progression. Here we demonstrate for the first time that circulating NET levels are elevated in advanced esophageal, gastric and lung cancer patients compared to healthy controls. Using pre-clinical murine models of lung and colon cancer in combination with intravital video microscopy, we show that NETs functionally regulate disease progression and that blocking NETosis through multiple strategies significantly inhibits spontaneous metastasis to the lung and liver. Further, we visualize how inhibiting tumor-induced NETs decreases cancer cell adhesion to liver sinusoids following intrasplenic injection – a mechanism previously thought to be driven primarily by exogenous stimuli. Thus, in addition to neutrophil abundance, the functional contribution of NETosis within the TIME has critical translational relevance and represents a promising target to impede metastatic dissemination.

Primary tumors induce neutrophil extracellular traps with targetable metastasis promoting effects

Roni F. Rayes[1,*], Jack G. Mouhanna[1,*], Ioana Nicolau[2], France Bourdeau[1], Betty Giannias[1], Simon Rousseau[3], Daniela Quail[4], Logan Walsh[4], Veena Sangwan[1], Nicholas Bertos[1], Jonathan Cools-Lartigue[1], Lorenzo E. Ferri[1], Jonathan D. Spicer[1].

[1]Cancer Research Program and the LD MacLean Surgical Research Laboratories, Department of Surgery, McGill University Health Center, Montreal, QC, Canada; [2]Dalla Lana School of Public Health, University of Toronto, Toronto, ON, Canada; [3]Meakins-Christie Laboratories, Department of Medicine, McGill University and the McGill University Health Center, Montreal, QC, Canada; [4]Goodman Cancer Research Center, McGill University, Montreal, QC, Canada.

* RFR and JGM equally contributed to the paper – co-first authorship.

The authors have declared that no conflict of interest exists

Corresponding Author: Jonathan D. Spicer

Montreal General Hospital, Room L8-505 - 1650 Cedar Avenue, Montreal, QC, Canada H3G 1A4; Phone: (514) 934-1934 ext 43050; E-mail: jonathan.spicer@mcgill.ca.

Abstract

Targeting the dynamic tumor immune microenvironment (TIME) can provide effective therapeutic strategies for cancer. Neutrophils are the predominant leukocyte population in mice and humans, and mounting evidence implicates these cells during tumor growth and metastasis. Neutrophil extracellular traps (NETs) are networks of extracellular neutrophil DNA fibers that are capable of binding tumor cells to support metastatic progression. Here we demonstrate for the first time that circulating NET levels are elevated in advanced esophageal, gastric and lung cancer patients compared to healthy controls. Using pre-clinical murine models of lung and colon cancer in combination with intravital video microscopy, we show that NETs functionally regulate disease progression and that blocking NETosis through multiple strategies significantly inhibits spontaneous metastasis to the lung and liver. Further, we visualize how inhibiting tumor-induced NETs decreases cancer cell adhesion to liver sinusoids following intrasplenic injection – a mechanism previously thought to be driven primarily by exogenous stimuli. Thus, in addition to neutrophil abundance, the functional contribution of NETosis within the TIME has critical translational relevance and represents a promising target to impede metastatic dissemination.

Introduction

Metastasis remains the leading cause of death among cancer patients. The role of the tumor immune microenvironment (TIME) in cancer initiation, progression and treatment efficacy is well-established (1) and led to the development of cancer immunotherapies (2, 3). Granulocytic neutrophils, the most abundant leukocyte in mammals, are the first cells of the innate immune system to be recruited to inflammation sites. They have diverse cytotoxic functions due to high concentrations of proteases and reactive oxygen species within their granules, which encounter pathogens through phagocytosis, degranulation, or release of neutrophil extracellular traps (NETs). Paralleling a growing appreciation for the link between inflammation and cancer, we (4, 5) and others (6-10) have demonstrated a regulatory role for neutrophils during various stages of tumor initiation and metastatic progression.

NETs are neutrophil-derived webs of DNA decorated with granular proteins, including myeloperoxidase (MPO) and neutrophil elastase (NE), that were initially shown to capture and kill foreign pathogens (11-13). However, more recent studies have also shown a noninfectious role for NETosis (14). For example, our group was the first to demonstrate a role for NETs in cancer progression (15). We discovered that NETosis can be induced by sepsis, which in turn promotes metastatic progression by trapping circulating tumor cells and promoting their proliferation in secondary sites (15, 16). Additional studies have since reported similar findings, whereby cancer progression is potentiated by NETosis induced by LPS (17, 18), tobacco smoke (17), tumor-derived inflammatory cytokines (18-20), or surgical stress (21). These preclinical findings suggest that various types of systemic inflammatory insults may induce NETosis in

cancer patients to support advancement of disease. However, data that directly address the relevance of this phenomenon in human cancer patients is absent, and few validated biomarkers exist for the identification of patients that might benefit from NET-directed therapy.

Evidence for the presence of NETs in humans is focused largely on infection, tissue injury, and autoimmunity, with minimal data in cancer patients. For instance, elevated levels of circulating NETs are observed in blood of patients with inflammatory conditions (22-26) relative to healthy controls. These observations prompt the question of whether tumor-driven inflammation can induce NETs in the absence of infection. Indeed, it is only recently that NETs were thought to be involved in cancer progression and metastasis (reviewed in (27)). One group has shown that neutrophils isolated from colorectal cancer patients had increased NET production as compared to neutrophils isolated from age-matched healthy individuals following *in vitro* stimulation (28). Interestingly, NET levels were shown to be an independent prognostic factor in pancreatic ductal adenocarcinoma (29) and H3Cittrulline a good diagnostic and prognostic marker of cancer progression (30), showing the importance of NETs as biomarkers of cancer. Moreover, NETs were shown to facilitate ovarian cancer metastasis to the omentum (31), implicating NETs once again in cancer metastasis.

Our previous work has demonstrated a tumor-promoting role for NETs in preclinical models of cancer (15, 32). Here, we investigate whether circulating NET levels are elevated in patients with several high-lethality malignancies, including lung, esophageal and gastric adenocarcinoma, and show that higher NET level is associated with disease stage. Using preclinical models of lung and gastrointestinal cancer, we

confirm that tumors prime neutrophils to undergo NETosis in the absence of infection/surgical stress to promote metastatic progression. Further, these pro-tumorigenic NETs can be therapeutically exploited through both pharmacologic and genetic approaches. Importantly, our results show that higher NET levels in cancer patients can be used as a biomarker of progressive disease independent of neutrophil to lymphocyte ratio (NLR) or absolute neutrophil count - two gold-standard clinical biomarkers of cancer prognosis. This study is the one of the first to bring large-scale human data to the forefront for several important tumor sites and directly address the relevance of NETosis in human cancer. Therefore, our findings have critical implications for translating NET-directed therapies to clinical trial implementation.

Results

NET levels correlate with disease stage. To explore whether NETs are present in the circulation in human cancer patients, we used an MPO-dsDNA ELISA (referred to as NET ELISA) (22-24). The sensitivity and specificity of the NET ELISA were confirmed (Supplemental Figure 1A-E). Indeed, stimulating isolated human neutrophils with increasing concentrations of PMA (0.0625 μM to 2 μM) resulted in a dose-dependent increase in NET levels as detected by the NET ELISA (Supplemental Figure 1A). Sytox staining of those stimulated neutrophils confirmed that what the assay measures are NETs as seen using a fluorescent plate reader (Supplemental Figure 1B) and under a fluorescent microscope (Supplemental Figure 1C). In addition, we show that the ELISA is specific to NETs and does not measure any neutrophil or tumor DNA (Supplemental Figure 1D). Moreover, we show that NETs can be measured in plasma or serum from whole blood and that an increase in NETs following PMA stimulation or a decrease in NETs following DNase treatment can be detected by the NET ELISA (Supplemental Figure 1E). Following this validation, we measured circulating NET levels in the plasma of 60 treatment-naïve lung or upper GI (esophagogastric) adenocarcinoma patients compared to 15 healthy individuals. We observed a trend of higher level of circulating NETs in cancer patients with advanced cancer (stage III-IV esophagogastric and stage II-III lung) compared to healthy controls (p-value = 0.0265) and significantly higher NET levels in patients with advanced cancer (stage III-IV esophagogastric and stage II-III lung) compared to patients with local disease (stage I-II esophagogastric and stage I lung) (p-value = 0.009, Figure 1A; cohort demographics are presented in Table 1). There was no difference in NET levels between patients with local disease and healthy

controls (p-value=0.20, Figure 1A). Within the esophagogastric patients, NET levels were higher in patients with overall stage III-IV disease compared to stage I-II (p-value = 0.03, Figure 1B), T3-4 tumors compared to T1-2 (Supplemental Figure 2A), positive lymph node status compared to no lymph node involvement (Supplemental Figure 2B), and distant metastasis compared to non-metastatic tumors (Supplemental Figure 2C). Within the lung patients, NET levels were higher in patients with overall stage II-III disease compared to stage I (p-value = 0.05, Figure 1C) and T2+ tumors compared to T1 (Supplemental Figure 2D). Together, these data indicate that treatment and surgical stress are not required to induce NETosis in cancer patients (21) and that the presence of a tumor alone correlates with an increase in NET levels, suggesting that tumors can induce NETosis in the absence of any other stimuli.

Advanced cancer stage and diabetes are independent predictors of NET levels. We next wanted to determine whether NET levels could be used as a biomarker of cancer stage. Multivariable logistic regression analyses were performed on the cancer patient cohort to identify whether stage was an independent predictor of NET levels, adjusting for the following confounders: age, sex, BMI, comorbidity, smoking and diabetes. The analyses revealed that cancer stage and diabetes are a significant independent predictor of NET levels (Table 2). Moreover, while NET levels correlated with overall stage in both esophagogastric (Figure 1B) and lung (Figure 1C) patients, neutrophil-to-lymphocyte ratios (NLRs) did not correlate with overall stage in either patient group (Supplemental Figure 3A, C). NLRs did, however, correlate with T staging in both groups (Supplemental Figure 3B, D). Similarly, absolute neutrophil counts did

not correlate with overall stage (Supplemental Figure 4A, C) but did correlate with T staging (Supplemental Figure 4B, D). Finally, neither NLR nor absolute neutrophil count correlated with NET levels (Supplemental Figure 3E, 4E); however, as expected, absolute neutrophil count correlated with NLR (Supplemental Figure 4F). These findings indicate that NET levels are a strong prognostic factor of advanced stage cancer independent of NLR and neutrophil count. Therefore, NET levels may represent a more sensitive measure of cancer-related inflammation than more crude measures such as NLR that have been investigated extensively in the clinical literature.

NET levels are correlated with the presence and progression of primary lung tumors in preclinical models. To better delineate the functional contribution of NETs during cancer progression, we used immunocompetent syngeneic murine models of lung and GI cancer. We injected Lewis-lung carcinoma cells (H59) subcutaneously into the flank of C57BL/6 mice. We collected plasma from the peripheral blood of H59 tumor-bearing mice 1-2 weeks and 3-4 weeks post-tumor inoculation and compared the NET levels to those in non-tumor bearing mice (Figure 2A). We observed significantly higher circulating NET levels 3-4 weeks post-tumor injection compared to either non-tumor bearing mice or to tumor-bearing mice 1-2 weeks post-tumor injection (Figure 2B). Once the tumor reached ~1.5 cm^3, it was resected, and NET levels were assessed. We observed that within two days following tumor resection and up to the time of sacrifice (two weeks post-resection), NET levels fell back to their baseline levels prior to tumor inoculation (Figure 2B). These data recapitulate our findings in patients, by

demonstrating that NET levels are higher in the presence of a tumor compared to non-tumor bearing controls.

NET levels in tumor-bearing mice are decreased by DNAse1 treatment, by NE inhibition and in *Pad4-/-* mice. Next, we sought to assess the functional contribution of NETs to tumor progression, by treating tumor bearing mice with a NET degrading enzyme (DNase1) or a NET inhibitor (NEi, Sivelestat). We measured NET levels in these 2 treatment groups of mice 3-4 weeks post-H59-GFP lung tumor inoculation, when the tumor reached ~2 cm^3 and compared them to untreated tumor-bearing mice (Figure 2C). Tumor-bearing mice treated with DNase1 or NEi had significantly lower NET levels compared to untreated tumor-bearing mice (Figure 2D). These data suggest that NET-targeted therapies using a NET degrader, DNase1, or a NET inhibitor, NEi, can decrease circulating NET levels.

We also utilized genetically modified mice that lack peptidyl arginine deiminase type IV (PAD4), a key enzyme in NET formation (33), and thus are NET-deficient (Figure 2C). PAD4 is an important mediator of innate immunity since *PAD4-/-* mice were shown to be more vulnerable to bacterial infection (34). Moreover, it was recently shown that many known physiological NET inducers (fMLP, GM-CSF, TNFα, or PMA) are PAD4 dependent (35). Here again, we found that *PAD4-/-* tumor-bearing mice had significantly lower NET levels compared to untreated tumor-bearing mice (Figure 2D). Therefore, primary tumors induce NET release in a PAD4-dependent manner and PAD4-targeted therapies using PAD4 inhibitors can decrease circulating, tumor-induced, NET levels.

Neutrophils are more sensitized to NETose in tumor-bearing mice compared to NET-deficient mice. To assess whether neutrophils are more primed towards NETosis in the presence of cancer, we used imaging flow cytometry, which is a novel flow-based imaging technique to measure the nucleus size of circulating neutrophils as a surrogate for their activation state (36). A seminal event in NETosis is the decondensation of DNA prior to its release, resulting in a measurable increase in the size of the nucleus (36). We first validated this assay using isolated murine neutrophils stimulated with PMA compared to non-stimulated neutrophils. By quantifying the change in nuclear area in images of circulating neutrophils, we were able to infer the activation state of neutrophils (Supplemental Figure 5A and 3A). We observed that the median baseline nucleus area of neutrophils in tumor-bearing mice prior to stimulation (87±3 μm^2) was not significantly different compared to neutrophils from non-tumor-bearing mice (88±3 μm^2), NEi-treated tumor-bearing mice (87±1 μm^2), DNase1-treated tumor-bearing mice (84±2 μm^2) and *PAD4-/-* tumor-bearing mice (89±4 μm^2) (orange curves in Figure 3C; population selection is shown in Supplemental Figure 5B). However, neutrophils from tumor-bearing mice were more sensitive to PMA stimulation (500 nM, 1 hr; 10%±2 increase in nucleus size) than non-tumor-bearing mice (3%±1 increase). Blockade of NET formation in NEi-treated tumor-bearing mice (3%±1 increase) and *PAD4-/-* tumor-bearing mice (5%±1 increase) rescues the phenotype (Figure 3B-D). DNase1-treated tumor-bearing mice were not less sensitive than tumor-bearing mice (11%±1 increase; Figure 3B-D), a likely explanation being that DNase1 degrades NETs after they are produced and has no effect on nuclear decondensation. These data suggest that

primary tumors prime circulating neutrophils to release NETs and that NET inhibitors rescue this phenotype.

NET-deficient mice have reduced cancer cell adhesion to the liver. Previous studies have shown that neutrophils travel to the liver sinusoids and release NETs to capture bacteria from the bloodstream during sepsis (37). Given our previous findings that NETs facilitate liver metastasis (15), we next asked whether NETs were similarly capable of capturing cancer cells from circulation to facilitate liver metastasis in the absence of sepsis. We performed intravital microscopy (IVM) to measure *in vivo* adhesion of intrasplenically injected H59-GFP cells in tumor-bearing mice. We observed a significant increase in *in vivo* hepatic adhesion of intrasplenically injected cells in tumor-bearing mice compared to non-tumor-bearing mice, DNase1- or NEi-treated tumor-bearing mice and *PAD4-/-* tumor-bearing mice (Figure 4A-C). Since our initial analysis included patients with both lungs and GI cancers (Figure 1), as a complementary model, we also performed intrasplenic injection of the colon cancer cell line, MC38-RFP. We similarly observed a significant increase in *in vivo* hepatic adhesion of intrasplenically injected MC38-RFP in tumor-bearing mice compared to non-tumor-bearing mice, DNase1- or NEi-treated tumor-bearing mice and *PAD4-/-* tumor-bearing mice (Figure 4D, E). These data demonstrate that both lung and colon primary tumors induce NETs that promote adhesion of circulating tumor cells to the liver, even in the absence of sepsis.

NET-deficient mice have reduced spontaneous liver and lung metastasis. To assess whether the tumor-induced NETs affect tumor cell metastasis, we injected subcutaneously into the flank H59-GFP cells that have been previously shown to spontaneously metastasize to the lung and liver (38), two of the most common metastatic sites. To visualize liver and lung metastases in H59-GFP tumor-bearing mice, the primary tumor was resected when it reached ~1.5-2 cm^3 and mice were sacrificed after 2 weeks (Figure 5A). Numerous lung metastases were observed (> 300 tumor cells per lung) and were thus quantified by extracting and homogenizing the lung tissue and counting GFP+ tumor cells by flow cytometry. There was a marked reduction in spontaneous lung metastasis in the NET-deficient tumor-bearing mice, DNase1- or NEi-treated and *PAD4-/-* tumor-bearing mice, compared to untreated tumor-bearing mice (Figure 5B, C and Supplemental Figure 6).

To assess spontaneous liver metastasis formation, murine livers were extracted, and liver metastases were quantified using fluorescence microscopy once the flank lesions reached ~1.5 - 2 cm^3 (Figure 5D). Flow cytometry was not needed in this case as fewer cells metastasized to the liver as compared to lungs. We observed reduced spontaneous liver metastasis in NET-deficient tumor-bearing mice, DNase1- or NEi-treated and *PAD4-/-* tumor-bearing mice, compared to untreated tumor-bearing mice (Figure 5E, F).

Together, these data indicate that primary tumors can induce metastasis promoting NETs in the absence of sepsis and that NET-targeted therapies reduce both lung and liver metastasis.

Discussion

Inflammation and immune cell chemotaxis have been recognized as key players in cancer progression, and clinical and experimental evidence points to pro-tumorigenic roles for neutrophils. Neutrophils are stimulated to release pathogen-trapping NETs as an antimicrobial mechanism in response to infectious stimuli (11). We were the first to show that NETs trap CTCs in the microvasculature, increasing tumor adhesion and promoting metastasis in a murine model of postoperative infection (15). Here, we describe for the first time that NET levels are elevated in lung, gastric and esophageal cancer patients and that high levels of NETs are predictive of advanced disease. Furthermore, we find that cancer is an independent predictor of NET formation over other co-morbidities. Inhibiting or degrading NETs leads to decreased lung and colon cancer adhesion and metastasis in a murine model, suggesting that NET-targeted therapies may limit metastasis.

Besides tumor stage, diabetes was also an independent predictor of elevated NET levels. This result is consistent with previous work showing that neutrophils from diabetic patients are primed for NETosis (39) and that high NET levels are correlated with type 2 diabetes (40). In addition, there was a trend towards higher NET levels in patients with high BMI which is relevant given that obesity is associated with chronic, low-grade inflammation that can modulate the TIME (reviewed in (41)) and facilitate breast-cancer cell metastasis via increased neutrophil recruitment (42).

Several conditions that are known to induce extensive inflammation were shown to lead to an increase in NET levels in humans (21-26, 39, 40, 43). Here we show that in addition to those conditions, primary tumors alone, from multiple disease sites, and in

the absence of any infection, can induce NETs. This is not totally unexpected since one of the hallmarks of cancer is inflammation (44). Moreover, a recent preclinical study has shown that metastatic breast cancer cells can induce metastasis-supporting NETs in mice, where treatment with DNase1-coated nanoparticles reduced lung metastasis (20). This is in line with our findings that DNase 1 or NEi treatments decrease liver and lung metastasis. These seminal findings advocate for the development of clinical trials to determine whether NET-targeted therapies can reduce metastasis.

To date, there are no clinical trials to evaluate the effects of targeting NETs on cancer progression. There is only one Phase 1 pilot study assessing the effects of recombinant DNase1 in patients with head and neck cancers treated with radiation therapy and chemotherapy (NCT00536952). Although not a goal of the study, it would be interesting to see if DNase1 treatment will delay cancer progression and metastasis.

Our study shows that inhibition of NETs via either NEi or using *PAD4*$^{-/-}$ mice leads to a decrease in NET levels which translates into less *in vivo* adhesion of circulating tumor cells to the liver sinusoids and a decrease in spontaneous lung and liver metastasis, a similar effect seen when DNase is administrated in those mice. Since NE and PAD4 are implicated in different NETosis pathways (ROS-dependent and ROS-independent) and seeing that DNase treatment does not have a larger effect as compared to NE and PAD4 inhibition, this indicates that NEi and *PAD4*$^{-/-}$ act on the same pathway.

Moreover, despite having a NET-mediated systemic effect that is promoting tumor metastasis, we found that the primary tumors of our non-septic mouse models did not induce a massive systemic inflammatory signature as seen in our septic mouse model (15). Indeed, we do not observe a massive deposition of NETs in the secondary organs

(lungs and livers) of non-septic TBM (Supplementary Figure 7) as was seen in the CLP mice (15). In addition, we are able to detect NETs in the primary tumor (flank) (Supplemental Figure 7A) but not in either of the metastatic sites (Supplemental Figure 7A, B) of non-septic TBM. Therefore, unlike in a septic mouse model (15) where we were able to observe NET deposition in the lungs and livers of CLP mice (by IVM and IHC), here, in non-septic TBM, we were only able to detect NETs in circulation (by ELISA). In addition, circulating neutrophils are primed to NETose as seen using imaging flow cytometry, another indication that NETosis is occurring in those mice. Therefore, primary tumor induced NETs can promote tumor metastasis by trapping CTCs (as seen in (15)) or by other mechanisms such as promoting thrombosis (reviewed in (45)) for example.

Several preclinical studies have shown that NETs can induce tumor growth and metastasis. However, most of those studies were done in the context of a massive inflammation or infection, such as sepsis (15), surgical stress (21) and prolonged tobacco smoke (17). Here, we show that primary tumors are sufficient to induce metastasis promoting NETs. Moreover, our study establishes circulating NET levels as a tumor-induced and prognostically significant biomarker. The emerging concept that a patient's immune state both systemically and within the developing cancer is a critical factor underlying response to immunotherapy further underpins the importance of our findings. Indeed, developing an understanding of how circulating NET levels impact response to treatment in cancer patients will be of critical importance to future studies. Both Sivelestat (NE inhibitor) and DNase1 have been tested and used for treating several respiratory conditions in humans at similar or higher concentrations, and thus

safety and pharmacokinetics studies have already been performed (46, 47). This simplifies the process of initiating a phase II clinical trial in cancer patients with either agent. This study therefore advocates for the use of NET-based therapeutics in cancer treatment to limit metastasis from several malignancies.

In conclusion, with all recent publications linking elevated NET levels with the progression of several malignancies such as breast (20) and colorectal (28) cancer, pancreatic ductal adenocarcinoma (29), ovarian metastasis (31) and, here, lung and gastroesophageal adenocarcinoma, it is interesting to see how successful NET-targeted therapies will be in clinical trials and how helpful NET-based biomarkers will be in predicting and prognosticating cancer progression and metastasis.

Methods

Model building strategy for the multivariate analysis. The analysis was performed to identify whether NET absorbance is a significant independent predictor of disease progression (overall stage) and adjusting for important available confounders: age, sex, BMI, smoking, diabetes, and comorbidities. All confounders were chosen because they have been shown to induce NET release (39, 48, 49). Multivariable logistic regression analyses were performed, and model assumptions were tested using graphical representations of residuals, residuals versus main predictor variable graphs as well as residuals versus predicted variable graphs. Model fit was tested using the likelihood ratio test with nested models.

Clinical staging, instead of pathological, was used for esophagogastric adenocarcinomas given the downstaging effects of chemotherapy (50-52), with 1/3 patients receiving neoadjuvant chemotherapy and 1/5 having inoperable disease.

Cell lines. Murine Lewis Lung carcinoma cell subline H59, expressing stable GFP (H59-GFP), was a kind gift of Dr. Pnina Brodt (53) and maintained in RPMI supplemented with 10% FBS, 100 µg/mL Penicillin/Streptomycin and 300 µg/mL glutamine (Wisent Bioproducts). Murine colon carcinoma cell line MC38 was a kind gift of Dr. Nicole Beauchemin (54) and maintained in DMEM media supplemented with 10% FBS and 100 µg/mL Penicillin/Streptomycin. MC38-GFP and MC38-RFP were engineered by transduction of MC38 with viral particles containing GFP and RFP, respectively, according to manufacturer's instructions (CMV-Luciferase(firefly)-2A-GFP(Puro) and CMV-Luciferase(firefly)-2A-RFP(Puro) from GenTarget, San Diego, CA).

Animals. C57BL/6 (Charles River, St Constant, QC) and *PAD4* knock out (*PAD4-/-*; kind gift of Dr. Alan Tsung) male mice were used for all experiments at 7-10 weeks old. MC38-RFP and H59-GFP were injected subcutaneously into the flank of these mice and tumor growth monitored twice a week using a caliper. Mice were divided into untreated, daily intramuscular injection of 2.5 mg/kg DNase1 (Roche, Mississauga, ON), gavage of 2.2 mg/kg of Sivelestat (NEi, Abcam (Cambridge, MA)) and *PAD4-/-* mice.

Blood collection and processing. Human blood was obtained from consented patients and healthy volunteers as per lung (IRB#2014-1119) and esophageal/gastric (IRB#2007-856) biobanks. Mouse blood was collected by heart puncture from anesthetized mice. Human and mouse bloods were collected in heparinized tubes and centrifuged at 500g for 10 minutes at 4˚C. Plasma was collected and stored at -80˚C.

NETs ELISA. Immulon®4HBX 96-well plates (ThermoFisher Scientific, Waltham, MA) were coated with mouse or human MPO antibody (clone 266-6K1, 1:20, Hycult Biotechnology, Plymouth Meeting, PA) overnight at 4˚C. Wells were washed with PBS (wash step) and blocked with 1% BSA (Wisent Bioproducts) for 1 hour at room temperature (RT). Following a wash step, plasma was mixed with dsDNA-POD antibody (1:40, Cell death detection ELISA plus kit, Roche) and added to wells for 2 hours shaking at RT. Following a wash step, ABTS (Roche) was added for 30 minutes at 37˚C and the plate was read at 405 nm.

Neutrophil isolation from human peripheral blood. Human neutrophil isolation is described in (55).

Neutrophil isolation from mouse peripheral blood. Murine neutrophil isolation is similar to human neutrophil isolation, but neutrophils are stained with Ly6G prior to use.

Neutrophil isolation from mouse bone marrow. Mouse neutrophil isolation is described in (56).

Imaging flow cytometry (IFC). Peripheral blood neutrophils were isolated from mice with flank tumors sizes of 1.5-2cm^3 and fixed with 2% PFA then stained with DAPI (1:2000, ThermoFisher Scientific) and Ly6G-FITC (clone 1A8, 1:200, ThermoFisher Scientific). IFC was performed on an Amnis ImageStream MarkII (Millipore-Sigma).

Intravital video microscopy (IVM). Mice with H59-GFP or MC38-RFP tumor sizes of 1.5-2cm^3 were injected intrasplenically with 3x10^4 H59-GFP or MC38-GFP cancer cells, respectively, and adhesion to liver sinusoids visualized after 10 minutes as described in (15), using an LSM-780 confocal microscope (Carl Zeiss, Toronto, ON).

Flow cytometry. Lungs were excised from previously resected mice and minced using scissors, to which 10 mL of Liberase (Millipore-Sigma) in L-15 media (Wisent Bioproducts) were added and left shaking at 37˚C for 30 minutes. Homogenates were vigorously mixed and incubated for another 30 minutes shaking at 37˚C. Homogenates were strained through 70 μM filters, centrifuged at 480g for 5 minutes, resuspended in PBS and analyzed by flow cytometry for H59-GFP+ using FACScan and CellQuest Software for analysis (BD Biosciences).

Spontaneous liver metastasis from H59-GFP flank injected mice. Livers from H59-GFP flank injected mice were excised when the flank tumor size reached 2 cm^3 for non-resected mice and two weeks after resection for resected mice and hepatic nodules were counted under a fluorescent microscope.

Western Blot. Flank tumors, livers and lungs from C57BL/6 TBM were homogenized and protein extracted using RIPA buffer (ThermoFisher Scientific) as per manufacturer's instructions. Protein concentration was assessed using a BCA assay (Bio-Rad). 250 µg of cell lysates were loaded on a 12% SDS-PAGE and ran at 100V for 90 minutes at RT. Proteins were transferred onto a nitrocellulose membrane (Pall Corporation, Life Sciences) at 90V for 90 minutes in the cold room. Membranes were probed with H3Cit (abcam cat#5103, 1:1000) and β-actin (Sigma-Aldrich cat#A5441, 1:10,000) diluted in TBS-Tween (0.1%) for 1 hour at RT. Membranes were washed 3 times, 5 minutes each in TBST and then probed using HRP anti-rabbit (1:3,000) and HRP anti-mouse (1:2,000) (both from Jackson Immunoresearch laboratories) for H3Cit and β-actin, respectively. Membranes were incubated with Clarity Western ECL substrate (Bio-Rad) for 5 minutes prior to imaging using the LAS4000 ImageQuant (Perkin Elmer).

Immunofluorescence. Livers and lungs from C57BL/6 mice were fixed with formalin for 48 hours and then paraffin embedded. FFPE blocks were then sectioned and stained at the histopathology platform of the RI-MUHC. H3Cit (abcam cat#5103, 1:100) and Ly6G-AF647 (clone 1A8, Biolegend, 1:200) were used with a PE conjugated anti-rabbit antibody (Lifetechnologies) as a secondary for H3Cit. Images were acquired on a LSM780 laser scanning confocal microscope (Zeiss) using an EC Plan-Neofluar 10x/0.30 lens.

Statistics. A Shapiro-Wilk test was performed for each Figure to assess if our data are normally distributed. For normally distributed data, a student T-test and one-way ANOVA were performed to compare mean values between different groups. A Kruskal-

Wallis non-parametric test was used to assess statistical differences between the different groups. In all cases, a p-value less than 0.05 was considered significant.

Study approval. All mice experiments were carried out in strict accordance with the recommendations of the Canadian Council on Animal Care (CCAC) ‘‘Guide to the Care and Use of Experimental Animals’’ and under the conditions and procedures approved by the Animal Care Committee of McGill University (AUP # 7724). All clinical work was performed under the considerations and procedures approved by the McGill University Health Center (MUHC) Research Ethics Board (REB) (project number 2007-856 and 2014-1119). Written informed consent was received from participants prior to inclusion in the study.

Author Contributions

RFR and JGM conducted all the experiments, acquired and analyzed the data, and wrote the paper.

IN conducted the multivariate analysis.

FB helped conduct the *in vivo* experiments.

BG helped conduct the *in vitro* experiments.

SR, DQ, LW, VS, NB, JCL and LEF provided input and guidance.

JS planned, oversaw, and guided the project.

Funding:

- Canadian Institutes of Health Research (CIHR) to LF.
- American Association for Thoracic Surgery (AATS) to JS.
- Fonds de Recherche du Quebec - Sante (FRQS) to JS.

Acknowledgments

We would like to thank Dr. Min Fu (manager molecular imaging platform), Mrs. Marie Helene Lacombe (manager immunophenotyping platform) and Mrs. Fazila Chaouli (manager histopathology platforms) as well as all the staff members of those core facilities for their help in planning, operating, and analyzing all of our experiments.

REFERENCES

1. Binnewies M, Roberts EW, Kersten K, Chan V, Fearon DF, Merad M, Coussens LM, Gabrilovich DI, Ostrand-Rosenberg S, Hedrick CC, et al. Understanding the tumor immune microenvironment (TIME) for effective therapy. *Nat Med.* 2018;24(5):541-50.
2. Sharma P, and Allison JP. The future of immune checkpoint therapy. *Science.* 2015;348(6230):56-61.
3. Sharon E, Streicher H, Goncalves P, and Chen HX. Immune checkpoint inhibitors in clinical trials. *Chin J Cancer.* 2014;33(9):434-44.
4. McDonald B, Spicer J, Giannais B, Fallavollita L, Brodt P, and Ferri LE. Systemic inflammation increases cancer cell adhesion to hepatic sinusoids by neutrophil mediated mechanisms. *Int J Cancer.* 2009;125(6):1298-305.
5. Spicer JD, McDonald B, Cools-Lartigue JJ, Chow SC, Giannias B, Kubes P, and Ferri LE. Neutrophils promote liver metastasis via Mac-1-mediated interactions with circulating tumor cells. *Cancer Res.* 2012;72(16):3919-27.
6. Singhal S, Bhojnagarwala PS, O'Brien S, Moon EK, Garfall AL, Rao AS, Quatromoni JG, Stephen TL, Litzky L, Deshpande C, et al. Origin and Role of a Subset of Tumor-Associated Neutrophils with Antigen-Presenting Cell Features in Early-Stage Human Lung Cancer. *Cancer Cell.* 2016;30(1):120-35.
7. Wculek SK, and Malanchi I. Neutrophils support lung colonization of metastasis-initiating breast cancer cells. *Nature.* 2015;528(7582):413-7.
8. Eruslanov EB, Bhojnagarwala PS, Quatromoni JG, Stephen TL, Ranganathan A, Deshpande C, Akimova T, Vachani A, Litzky L, Hancock WW, et al. Tumor-associated neutrophils stimulate T cell responses in early-stage human lung cancer. *J Clin Invest.* 2014;124(12):5466-80.
9. Tazzyman S, Lewis CE, and Murdoch C. Neutrophils: key mediators of tumour angiogenesis. *Int J Exp Pathol.* 2009;90(3):222-31.
10. Tuting T, and de Visser KE. CANCER. How neutrophils promote metastasis. *Science.* 2016;352(6282):145-6.
11. Brinkmann V, Reichard U, Goosmann C, Fauler B, Uhlemann Y, Weiss DS, Weinrauch Y, and Zychlinsky A. Neutrophil extracellular traps kill bacteria. *Science.* 2004;303(5663):1532-5.
12. Honda M, and Kubes P. Neutrophils and neutrophil extracellular traps in the liver and gastrointestinal system. *Nat Rev Gastroenterol Hepatol.* 2018;15(4):206-21.
13. Kolaczkowska E, Jenne CN, Surewaard BG, Thanabalasuriar A, Lee WY, Sanz MJ, Mowen K, Opdenakker G, and Kubes P. Molecular mechanisms of NET formation and degradation revealed by intravital imaging in the liver vasculature. *Nat Commun.* 2015;6(6673.
14. Jorch SK, and Kubes P. An emerging role for neutrophil extracellular traps in noninfectious disease. *Nat Med.* 2017;23(3):279-87.
15. Cools-Lartigue J, Spicer J, McDonald B, Gowing S, Chow S, Giannias B, Bourdeau F, Kubes P, and Ferri L. Neutrophil extracellular traps sequester circulating tumor cells and promote metastasis. *J Clin Invest.* 2013.
16. Cools-Lartigue J, Spicer J, Najmeh S, and Ferri L. Neutrophil extracellular traps in cancer progression. *Cell Mol Life Sci.* 2014;71(21):4179-94.

17. Albrengues J, Shields MA, Ng D, Park CG, Ambrico A, Poindexter ME, Upadhyay P, Uyeminami DL, Pommier A, Kuttner V, et al. Neutrophil extracellular traps produced during inflammation awaken dormant cancer cells in mice. *Science.* 2018;361(6409).
18. Demers M, Krause DS, Schatzberg D, Martinod K, Voorhees JR, Fuchs TA, Scadden DT, and Wagner DD. Cancers predispose neutrophils to release extracellular DNA traps that contribute to cancer-associated thrombosis. *Proc Natl Acad Sci U S A.* 2012;109(32):13076-81.
19. Demers M, Wong SL, Martinod K, Gallant M, Cabral JE, Wang Y, and Wagner DD. Priming of neutrophils toward NETosis promotes tumor growth. *Oncoimmunology.* 2016;5(5):e1134073.
20. Park J, Wysocki RW, Amoozgar Z, Maiorino L, Fein MR, Jorns J, Schott AF, Kinugasa-Katayama Y, Lee Y, Won NH, et al. Cancer cells induce metastasis-supporting neutrophil extracellular DNA traps. *Sci Transl Med.* 2016;8(361):361ra138.
21. Tohme S, Yazdani HO, Al-Khafaji AB, Chidi AP, Loughran P, Mowen K, Wang Y, Simmons RL, Huang H, and Tsung A. Neutrophil Extracellular Traps Promote the Development and Progression of Liver Metastases after Surgical Stress. *Cancer Res.* 2016;76(6):1367-80.
22. Kessenbrock K, Krumbholz M, Schonermarck U, Back W, Gross WL, Werb Z, Grone HJ, Brinkmann V, and Jenne DE. Netting neutrophils in autoimmune small-vessel vasculitis. *Nat Med.* 2009;15(6):623-5.
23. Sur Chowdhury C, Giaglis S, Walker UA, Buser A, Hahn S, and Hasler P. Enhanced neutrophil extracellular trap generation in rheumatoid arthritis: analysis of underlying signal transduction pathways and potential diagnostic utility. *Arthritis Res Ther.* 2014;16(3):R122.
24. Caudrillier A, Kessenbrock K, Gilliss BM, Nguyen JX, Marques MB, Monestier M, Toy P, Werb Z, and Looney MR. Platelets induce neutrophil extracellular traps in transfusion-related acute lung injury. *J Clin Invest.* 2012;122(7):2661-71.
25. Fuchs TA, Brill A, and Wagner DD. Neutrophil extracellular trap (NET) impact on deep vein thrombosis. *Arterioscler Thromb Vasc Biol.* 2012;32(8):1777-83.
26. Arai Y, Yamashita K, Mizugishi K, Watanabe T, Sakamoto S, Kitano T, Kondo T, Kawabata H, Kadowaki N, and Takaori-Kondo A. Serum neutrophil extracellular trap levels predict thrombotic microangiopathy after allogeneic stem cell transplantation. *Biol Blood Marrow Transplant.* 2013;19(12):1683-9.
27. Erpenbeck L, and Schon MP. Neutrophil extracellular traps: protagonists of cancer progression? *Oncogene.* 2017;36(18):2483-90.
28. Richardson JJR, Hendrickse C, Gao-Smith F, and Thickett DR. Neutrophil Extracellular Trap Production in Patients with Colorectal Cancer In Vitro. *Int J Inflam.* 2017;2017(4915062.
29. Jin W, Xu HX, Zhang SR, Li H, Wang WQ, Gao HL, Wu CT, Xu JZ, Qi ZH, Li S, et al. Tumor-Infiltrating NETs Predict Postsurgical Survival in Patients with Pancreatic Ductal Adenocarcinoma. *Ann Surg Oncol.* 2019;26(2):635-43.
30. Thalin C, Lundstrom S, Seignez C, Daleskog M, Lundstrom A, Henriksson P, Helleday T, Phillipson M, Wallen H, and Demers M. Citrullinated histone H3 as a

novel prognostic blood marker in patients with advanced cancer. *PLoS One.* 2018;13(1):e0191231.
31. Lee W, Ko SY, Mohamed MS, Kenny HA, Lengyel E, and Naora H. Neutrophils facilitate ovarian cancer premetastatic niche formation in the omentum. *J Exp Med.* 2019;216(1):176-94.
32. Najmeh S, Cools-Lartigue J, Rayes RF, Gowing S, Vourtzoumis P, Bourdeau F, Giannias B, Berube J, Rousseau S, Ferri LE, et al. Neutrophil extracellular traps sequester circulating tumor cells via beta1-integrin mediated interactions. *Int J Cancer.* 2017;140(10):2321-30.
33. Hemmers S, Teijaro JR, Arandjelovic S, and Mowen KA. PAD4-mediated neutrophil extracellular trap formation is not required for immunity against influenza infection. *PLoS One.* 2011;6(7):e22043.
34. Li P, Li M, Lindberg MR, Kennett MJ, Xiong N, and Wang Y. PAD4 is essential for antibacterial innate immunity mediated by neutrophil extracellular traps. *J Exp Med.* 2010;207(9):1853-62.
35. Tatsiy O, and McDonald PP. Physiological Stimuli Induce PAD4-Dependent, ROS-Independent NETosis, With Early and Late Events Controlled by Discrete Signaling Pathways. *Front Immunol.* 2018;9(2036.
36. Zhao W, Fogg DK, and Kaplan MJ. A novel image-based quantitative method for the characterization of NETosis. *J Immunol Methods.* 2015;423(104-10.
37. McDonald B, Urrutia R, Yipp BG, Jenne CN, and Kubes P. Intravascular neutrophil extracellular traps capture bacteria from the bloodstream during sepsis. *Cell Host Microbe.* 2012;12(3):324-33.
38. Brodt P. Characterization of two highly metastatic variants of Lewis lung carcinoma with different organ specificities. *Cancer Res.* 1986;46(5):2442-8.
39. Wong SL, Demers M, Martinod K, Gallant M, Wang Y, Goldfine AB, Kahn CR, and Wagner DD. Diabetes primes neutrophils to undergo NETosis, which impairs wound healing. *Nat Med.* 2015;21(7):815-9.
40. Menegazzo L, Ciciliot S, Poncina N, Mazzucato M, Persano M, Bonora B, Albiero M, Vigili de Kreutzenberg S, Avogaro A, and Fadini GP. NETosis is induced by high glucose and associated with type 2 diabetes. *Acta Diabetol.* 2015;52(3):497-503.
41. Olson OC, Quail DF, and Joyce JA. Obesity and the tumor microenvironment. *Science.* 2017;358(6367):1130-1.
42. Quail DF, Olson OC, Bhardwaj P, Walsh LA, Akkari L, Quick ML, Chen IC, Wendel N, Ben-Chetrit N, Walker J, et al. Obesity alters the lung myeloid cell landscape to enhance breast cancer metastasis through IL5 and GM-CSF. *Nat Cell Biol.* 2017;19(8):974-87.
43. Itagaki K, Kaczmarek E, Lee YT, Tang IT, Isal B, Adibnia Y, Sandler N, Grimm MJ, Segal BH, Otterbein LE, et al. Mitochondrial DNA released by trauma induces neutrophil extracellular traps. *PLoS One.* 2015;10(3):e0120549.
44. Hanahan D, and Weinberg RA. Hallmarks of cancer: the next generation. *Cell.* 2011;144(5):646-74.
45. Cedervall J, and Olsson AK. Immunity Gone Astray - NETs in Cancer. *Trends Cancer.* 2016;2(11):633-4.

46. Kido T, Muramatsu K, Yatera K, Asakawa T, Otsubo H, Kubo T, Fujino Y, Matsuda S, Mayumi T, and Mukae H. Efficacy of early sivelestat administration on acute lung injury and acute respiratory distress syndrome. *Respirology.* 2017;22(4):708-13.
47. Shak S, Capon DJ, Hellmiss R, Marsters SA, and Baker CL. Recombinant human DNase I reduces the viscosity of cystic fibrosis sputum. *Proc Natl Acad Sci U S A.* 1990;87(23):9188-92.
48. Qiu SL, Zhang H, Tang QY, Bai J, He ZY, Zhang JQ, Li MH, Deng JM, Liu GN, and Zhong XN. Neutrophil extracellular traps induced by cigarette smoke activate plasmacytoid dendritic cells. *Thorax.* 2017;72(12):1084-93.
49. Wang H, Wang Q, Venugopal J, Wang J, Kleiman K, Guo C, and Eitzman DT. Obesity-induced Endothelial Dysfunction is Prevented by Neutrophil Extracellular Trap Inhibition. *Sci Rep.* 2018;8(1):4881.
50. Andriessen MJ, van der Peet DL, and Cuesta MA. Effect of neoadjuvant chemotherapy on circumferential margin positivity and its impact on prognosis in patients with resectable oesophageal cancer (Br J Surg 2008; 95: 191-194). *Br J Surg.* 2008;95(10):1305-6; author reply 6.
51. Matsuyama J, Doki Y, Yasuda T, Miyata H, Fujiwara Y, Takiguchi S, Yamasaki M, Makari Y, Matsuura N, Mano M, et al. The effect of neoadjuvant chemotherapy on lymph node micrometastases in squamous cell carcinomas of the thoracic esophagus. *Surgery.* 2007;141(5):570-80.
52. Sujendran V, Wheeler J, Baron R, Warren BF, and Maynard N. Effect of neoadjuvant chemotherapy on circumferential margin positivity and its impact on prognosis in patients with resectable oesophageal cancer. *Br J Surg.* 2008;95(2):191-4.
53. Auguste P, Fallavollita L, Wang N, Burnier J, Bikfalvi A, and Brodt P. The host inflammatory response promotes liver metastasis by increasing tumor cell arrest and extravasation. *Am J Pathol.* 2007;170(5):1781-92.
54. Arabzadeh A, Chan C, Nouvion AL, Breton V, Benlolo S, DeMarte L, Turbide C, Brodt P, Ferri L, and Beauchemin N. Host-related carcinoembryonic antigen cell adhesion molecule 1 promotes metastasis of colorectal cancer. *Oncogene.* 2013;32(7):849-60.
55. Najmeh S, Cools-Lartigue J, Giannias B, Spicer J, and Ferri LE. Simplified Human Neutrophil Extracellular Traps (NETs) Isolation and Handling. *J Vis Exp.* 201598).
56. Mocsai A, Zhang H, Jakus Z, Kitaura J, Kawakami T, and Lowell CA. G-protein-coupled receptor signaling in Syk-deficient neutrophils and mast cells. *Blood.* 2003;101(10):4155-63.

Tables

Table 1. Demographics and clinical characteristics of cancer patients and healthy individuals.

	Patients with esophagogastric adenocarcinoma (n=37)	Patients with lung adenocarcinoma (n=23)	Healthy individuals (n=15)
Sex			
Male	25	15	8
Female	12	8	7
Age			
Mean ± SEM	68 ± 2	69 ± 2	31 ± 3
Range	39 - 94	49 - 85	23 - 53
Overall Stage			
I	5	16	-
II	7	4	-
III	17	3	-
IV	8	0	-
T Stage			
T1	5	9	-
T2	2	8	-
T3	22	5	-
T4	8	1	-
Lymph Node Status (N Stage)			
N0	14	21	-
N+	23	2	-
Distant Metastasis (M)			
M0	29	23	-
M1	8	0	-
BMI			
Mean ± SEM	27 ± 5	26 ± 5	-
Smoking Status			
Ever smoked	15	18	-
Charlson Comorbidity Index			
1	1	1	-
2	9	3	-
3	6	3	-

4	10	6	-
5	4	5	-
6	6	4	-
7	1	1	-
Diabetes			
Diabetic	7	5	-

Table 2. Multivariable logistic regression models to predict NET levels.

Variable	Multivariable model OR (95% CI)	p-value
Stage	0.138 (0.022 – 0.254)	**0.020**
Age	-0.0015 (-0.011 – 0.008)	0.76
Sex (M vs F)	0.098 (-0.025 – 0.221)	0.12
BMI	-0.012 (-0.026 – 0.001)	0.07
Charlson comorbidity index	-0.034 (-0.114 – 0.046)	0.405
Smoking (ever vs never)	-0.046 (-0.162 – 0.070)	0.436
Diabetes	0.313 (0.148 – 0.479)	**0.001**

Figures & Figure Legends

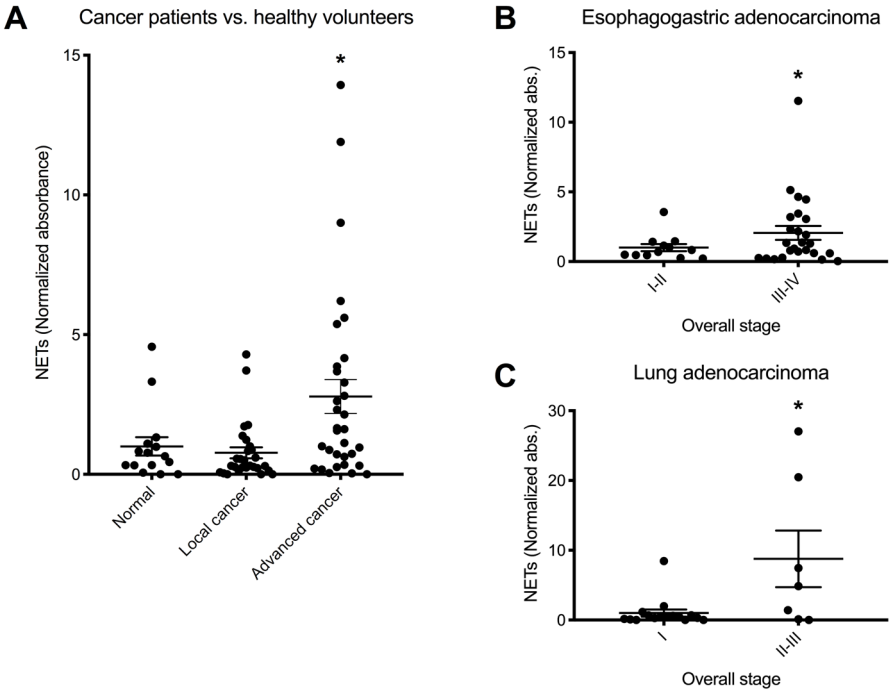

Figure 1. **Circulating NET levels in esophagogastric and lung adenocarcinoma patients. A.** NET levels (normalized to the average NET level of healthy individuals, labeled as normal) obtained by the NETs ELISA are shown for patients with local cancer (n=28) compared to patients with advanced cancer (n=32) compared to healthy individuals (labeled as normal; n=15). A Kruskal-Wallis test was used to calculate significance because the data were not normally distributed as assessed by the Kolmogorov-Smirnov test. **B.** NET levels (normalized to the average NET level of overall stage I-II) for esophagogastric adenocarcinoma patients are shown for overall stage I-II (n=12) and III-IV (n=25). **C.** NET levels (normalized to the average NET level of overall stage I) for lung adenocarcinoma patients shown plotted for overall stage I (n=16) and II-III (n=7). A student T-test was used to assess statistical significance for panels B and C. Mean ± SEM is shown for all panels. * $p<0.05$.

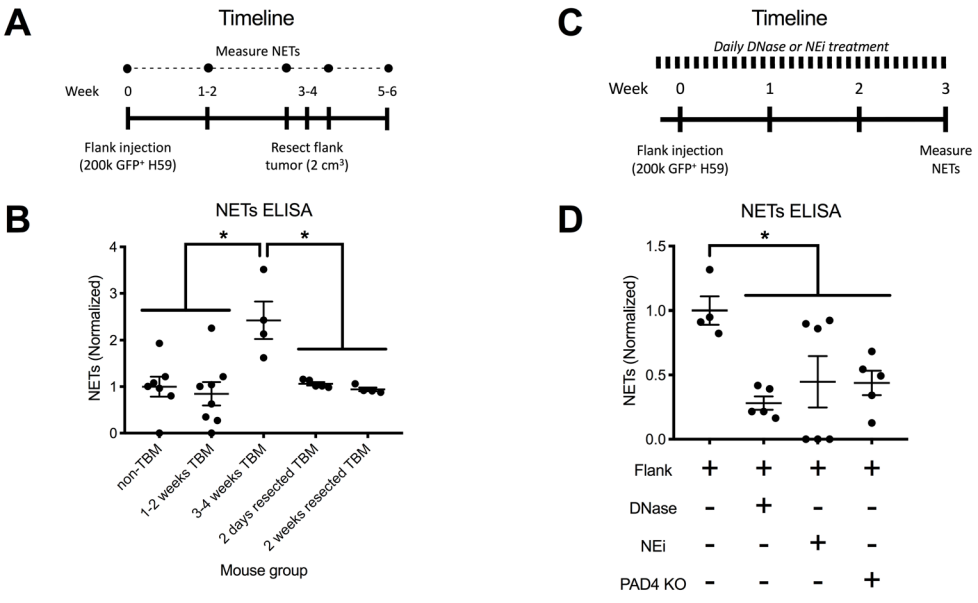

Figure 2. Circulating NET levels are decreased in tumor-bearing mice (TBM) following tumor resection or treatment with a NET inhibitor or degrader and in *PAD4-/-* TBM with inhibited NET formation. A. Timeline of murine lung carcinoma NET measurements. **B.** Mean (± SEM) NET levels (normalized to non-TBM) are shown for non-TBM (n=7), TBM 1-2 weeks (n=8) and 3-4 weeks (n=4) post-tumor inoculation, as well as TBM 2 days (n=5) and 2 weeks (n=4) post-resection. **C.** Timeline of the murine lung carcinoma NET measurements. **D.** Mean (± SEM) NET levels (normalized to TBM) are shown for TBM (n=4), TBM treated with DNase1 (n=5) or NEi (n=6) and *PAD4-/-* TBM (n=5). One-way ANOVA was used to assess statistical significance for panels B and D. * $p<0.05$.

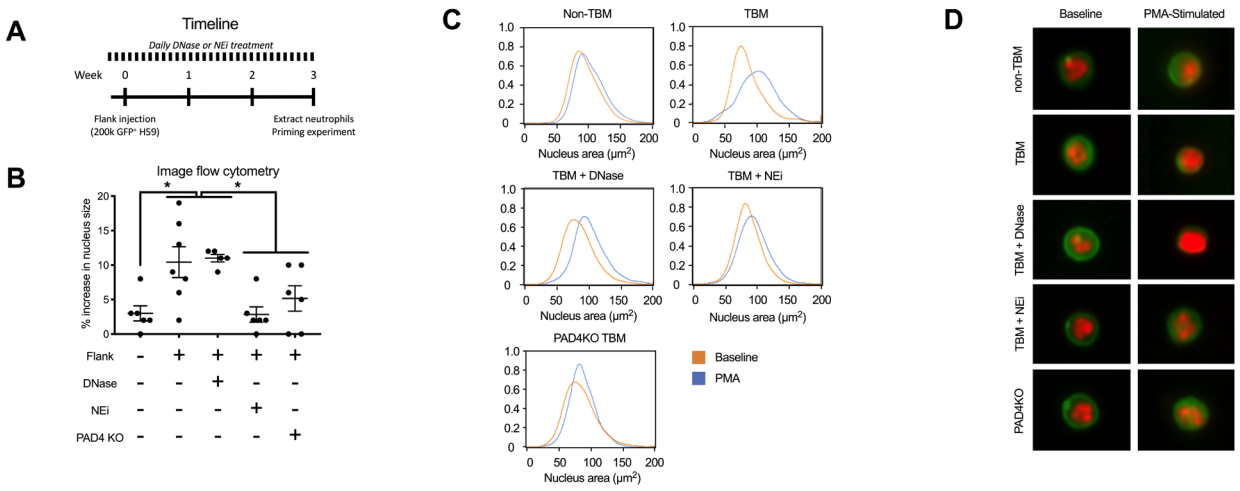

Figure 3. Neutrophils from TBM are more sensitized to NETosis compared to TBM treated with a NET inhibitor and in mice with inhibited NET formation. A. Timeline of murine lung carcinoma priming experiment. **B.** Bar graph of the mean (± SEM) percent change in nuclear area following PMA stimulation for non-TBM (n=6), TBM (n=7), TBM treated with DNase1 (n=6) or NEi (n=6) and *PAD4-/-* TBM (n=6). One-way ANOVA was used to assess statistical significance. * $p<0.05$. **C.** Representative histograms of the distribution of neutrophil nuclear area in the 5 group of mice from panel B are plotted at baseline (orange curve) and following PMA stimulation (blue curve). **D.** Representative images of neutrophils from the 5 groups of mice from panels B and C at baseline and after stimulation. Neutrophils are stained with Ly6G (green); nuclei are stained with DAPI (orange).

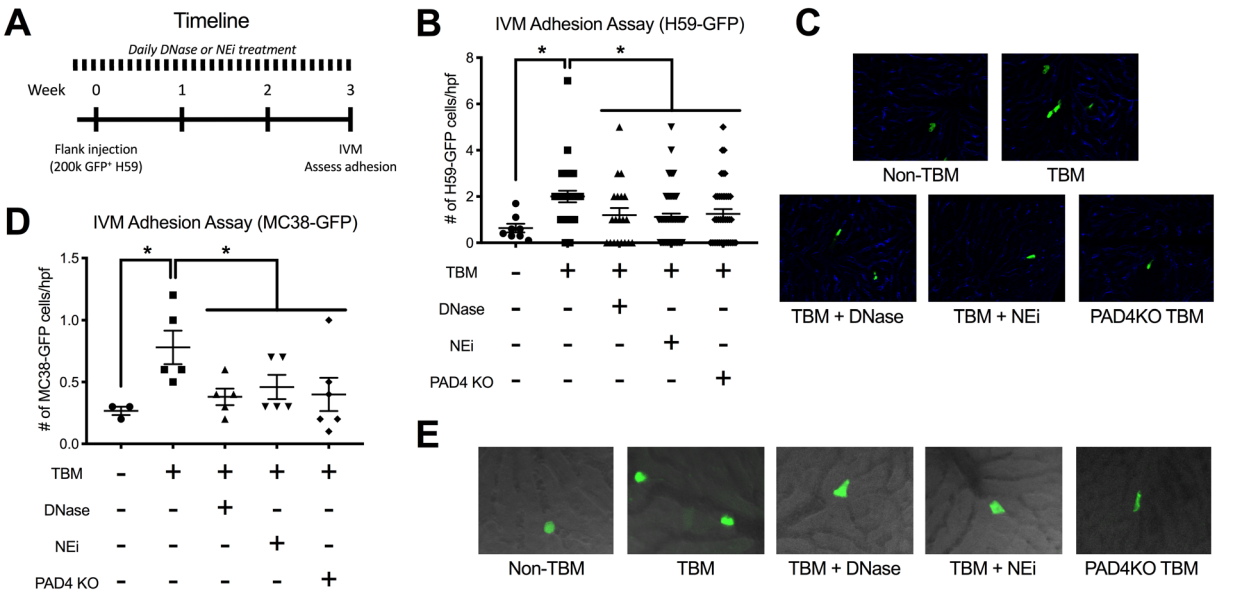

Figure 4. NET-deficient mice show reduced lung and colon cancer cell adhesion to the liver. A. Timeline of murine intravital microscopy (IVM) experiment. **B.** Mean (± SEM) number of adherent lung carcinoma cells (H59-GFP) per field in the 5 groups of mice from Figure 4. **C.** Representative fluorescence confocal microscopy images of IVM performed on the mice from panel B, showing H59-GFP cells in green; liver sinusoids are shown in blue (CD31-PE staining). **D.** Mean (± SEM) number of adherent colon carcinoma cells (MC38-GFP) per field in the 5 groups of mice from Figure 4. **E.** Representative fluorescence confocal microscopy images of IVM performed on the mice from panel D, showing MC38-GFP cells in green; liver sinusoids are shown using bright field. For all panels: n=3-6 mice, with 10 fields per mouse. A Kruskal-Wallis test was used to calculate significance for panels B and D because the data were not normally distributed as assessed by the Kolmogorov-Smirnov test. * $p<0.05$.

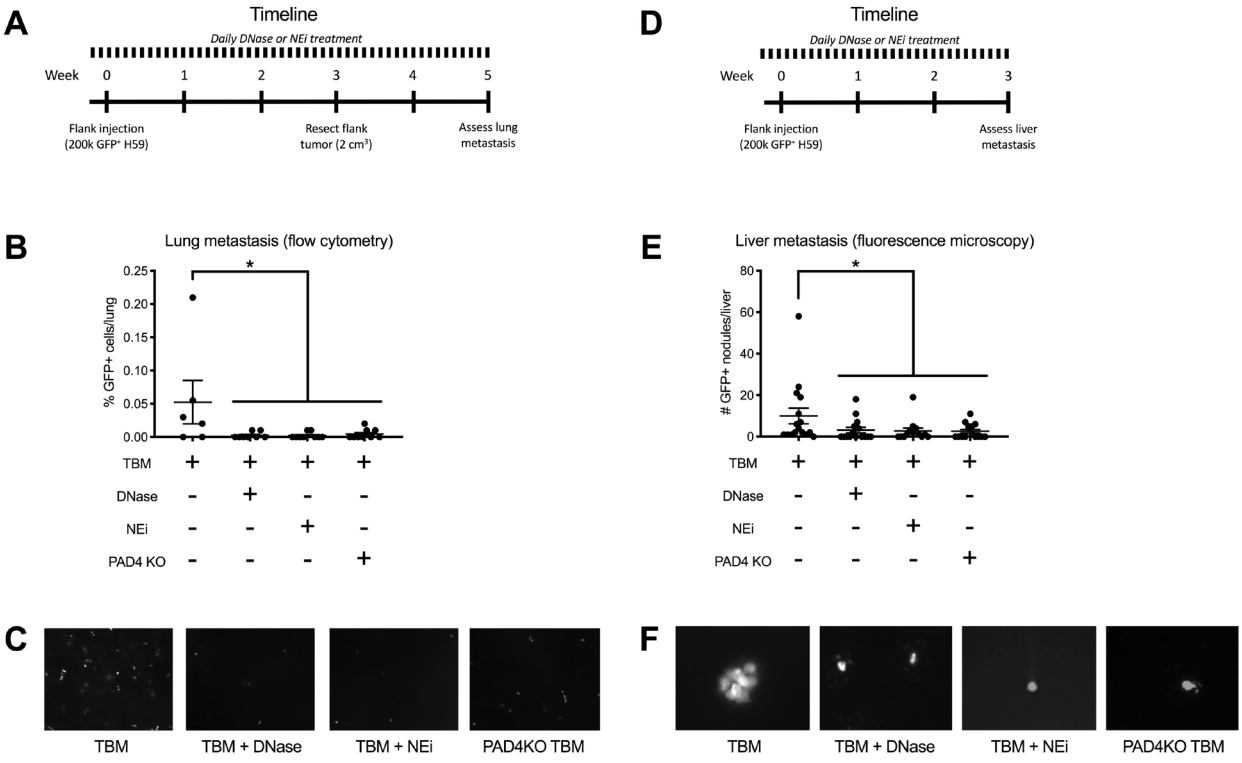

Figure 5. NET-deficient mice show reduced spontaneous lung and liver metastasis of lung carcinoma cells. A. Timeline of the murine spontaneous liver and lung metastasis experiment with resection. **B.** Mean (± SEM) % of H59-GFP+ cells in the lungs of TBM (n=6) and DNase1-treated (n=6), NEi-treated (n=9) and *PAD4-/-* (n=8) TBM. **C.** Representative fluorescence microscopy images of spontaneous lung metastases in the 4 groups of mice from panel B. **D.** Timeline of the murine spontaneous liver metastasis experiment without resection. **E.** Mean (± SEM) number of H59-GFP+ cells in livers of TBM (n=16) and DNase1-treated (n=15), NEi-treated (n=13) and *PAD4-/-* (n=15) TBM. **F.** Representative fluorescence microscopy images of spontaneous liver metastases in the 4 groups of mice from F. A Kruskal-Wallis test was used to calculate significance for panels B and E because the data were not normally distributed as assessed by the Kolmogorov-Smirnov test. * $p<0.05$.